In-Situ Measurement of Ionospheric E-Region Plasma Irregularities over Taiwan

Chi-Kuang Chao[1,2,*], Yen-Hsyang Chu[1,3], Ching-Lun Su[1], and Shigeyuki Minami[4]

[1] *Institute of Space Science, National Central University, Jhongli, Taiwan, ROC*
[2] *Department of Atmospheric Sciences, National Central University, Jhongli, Taiwan, ROC*
[3] *Center for Space and Remote Sensing Research, National Central University, Jhongli, Taiwan, ROC*
[4] *Faculty of Engineering, Osaka City University, Osaka, Japan*

ABSTRACT

One ion trap (IT) and one retarding potential analyzer (RPA) onboard the Taiwan Sounding Rocket V (SR-V) were launched to measure ionospheric plasma irregularities on 18 January 2006. After the fairing separated, voltage readings (V_{G1}) of the first grid (G1) in the IT indicated abnormally high negative voltages appeared at the upleg between 83.7 and 120.1 km altitude for 19.7 seconds. It is postulated G1 had temporarily shorted out with the other two grids. Such the anomaly in the V_{G1} brought out the expansion of a plasma sheath around opening of the IT. More ions were attracted into the collector. Remarkable ion currents detected by the IT led to malfunctions of the RPA simultaneously. In this article, laboratory simulations and the International Reference Ionosphere model are performed to evaluate scale factors for the IT to the anomaly. The calibrated total ion concentration profile at the upleg indicates a peak density of the E_s layer at 93.0 km altitude of about 6.9×10^3 # cm^{-3} with a thickness of 3.4 km. It is very similar to that at the downleg. It implies that the SR-V might encounter the same E_s layer twice in a distance of 150 km away.

Key words: Ion probe, Sounding rocket, Laboratory simulation, and Plasma chamber
Citation: Chao, C. K., Y. H. Chu, C. L. Su, and S. Minami, 2012: In-situ measurement of ionospheric E-region plasma irregularities over Taiwan. Terr. Atmos. Ocean. Sci., 23, 333-342, doi: 10.3319/TAO.2011.12.23.01(AA)

1. INTRODUCTION

Taiwan began a sounding rocket program in 1997. The National Space Organization (NSPO) is responsible for supporting the development of sounding rocket technologies. Local universities provide payloads for scientific research and engineering demonstrations. The Chungshan Institute of Science and Technology (CSIST) provides fabrication and sounding rocket launch services for science missions on demand. In the first phase three sounding rockets (code-named as SR-I, SR-II, and SR-III) were launched to demonstrate the capacity for academic study before the end of 2003. In the second phase 10 to 15 sounding rockets were planned for launch over the following 15 years. To date, the SR-IV, SR-V, SR-VI, and SR-VII have been launched. The missions include scientific research like neutral wind measurement by releasing trimethylaluminum (Chu et al. 2007)

from the SR-II and SR-III, ionospheric airglow studies in the SR-IV, plasma irregularities in the SR-V and SR-VII and engineering demonstrations using GPS receivers in the SR-IV, reusable capsules in the SR-VI, and hydrazine propulsion experiments in the SR-VI.

The Ion probe was used primarily to measure the ion temperature and concentrations in laboratory and was then deployed in many early space exploration programs (Boyd 1968). A planar multiple-grid type of ion probe was developed to be installed on many satellite missions, like the Injun 4 and 5, OGO 2, 4, and 6, AEROS A and B, Atmosphere Exlporer C, D, and E, Dynamic Explorer 1 and 2, San Marco-D/L. Special Sensors-Ions, Electrons, and Scintillation installed in the Defense Meteorological Satellite Program series (Heelis and Hanson 1998), Ionospheric Plasma and Electrodynamics Instrument on the first satellite of Republic of China (Yeh et al. 1999), and Ion Velocity Meter on Communication/Navigation Outage Forecasting System (de

---

* *Corresponding author*
  E-mail: ckchao@jupiter.ss.ncu.edu.tw

La Beaujardière et al. 2004) were all equipped with the similar ion probes.

Two planar-type ion probes were installed inside the fairing section of the Taiwan's Sounding Rocket V (SR-V) to measure ionospheric E-region plasma irregularities over Taiwan. One of the probes is configured as an ion trap (IT) and the other is a retarding potential analyzer (RPA). Each probe has an 88 mm diameter opening, three stainless steel T316 woven grids (50 meshes per inch and 0.05 mm diameter wires), and a collector connected to a current meter (see Fig. 1). Each grid is separated at a distance of 4 mm. The distance between the last grid and the collector is 3 mm.

The first grid arranged in the opening of the probe is an aperture grid (G1). Potential of the G1 is electrically isolated with other parts and is supposed to measure a floating potential which varies with the plasma potential under a net current balance. The G1 maintains a uniform electric potential plane to allow plasma coming into the probe smoothly without traversing an electric field. Potential differences (V_{G1}) between the G1 of the IT and the rocket ground are recorded. In normal operation, the V_{G1} are close to zero if the G1 is isolated from plasma. If the G1 contacts with the plasma, the V_{G1} go positive (but less than 1 V in most of the sounding rocket experiments) and increase with plasma density. The second grid arranged behind the G1 is called a retarding grid (G2). In the IT, the potential of the G2 also floats with the plasma potential similar to the V_{G1}. However, in the RPA, a feedback circuit provides a 10-Hz square wave, where V_{G2}, is also called a retarding voltage, on the G2 to regulate collector currents of the RPA to levels between 1/5 and 1/10 of the IT (Minami et al. 1982). The V_{G2} of the RPA are recorded and can be used to derive ion temperature by a graphical analysis method in the high sampling rate. The last grid (G3) is a suppressor and biased to -15 V to repel all incoming electrons away from the collector. The collector is a 68-mm diameter circular copper plate biased to -9 V as its surrounding guarding ring. Currents can be detected when the incoming ions finally hit the collector. The collector currents (I_{IT}) of the IT are recorded and their noise levels are below 0.2 nA.

If the I_{IT} are too small (less than a threshold level ~0.4 nA), the feedback circuit of the RPA cannot be triggered and the V_{G2} are always at -10 V. If the I_{IT} are higher than 2 nA (a stable level), the V_{G2} become stable. If the I_{IT} fall between the threshold and the stable levels, the V_{G2} are triggered to higher than -10 V but fluctuate randomly. It can be realized that both the 1/5 and 1/10 of the I_{IT} in stable level are just above the noise level of the current meters. If the V_{G2} are always at +10 V, it implies that the currents (I_{RPA}) measured by the RPA are lower than the 1/10 of the I_{IT}. Of course, all the voltages are again referenced to the rocket ground, which is connected to the metal body of the rocket.

In this article, the ion currents collected by the IT of the SR-V are shown first. Extraordinarily high currents are found when the SR-V passes through the E region at the upleg, but there are no reasonable readings available in the V_{G2} at that time. However, an anomaly in the V_{G1} emerges simultaneously as the extraordinary currents. Laboratory simulations are performed to evaluate possible responses of the IT to the anomaly. The extraordinary currents are mainly caused by a plasma sheath expansion around the IT opening. Scale factors estimated from the laboratory simulations and the International Reference Ionosphere model can be used to restore the E-region total ion concentration profile over Taiwan.

2. FLIGHT RESULTS OF SOUNDING ROCKET V

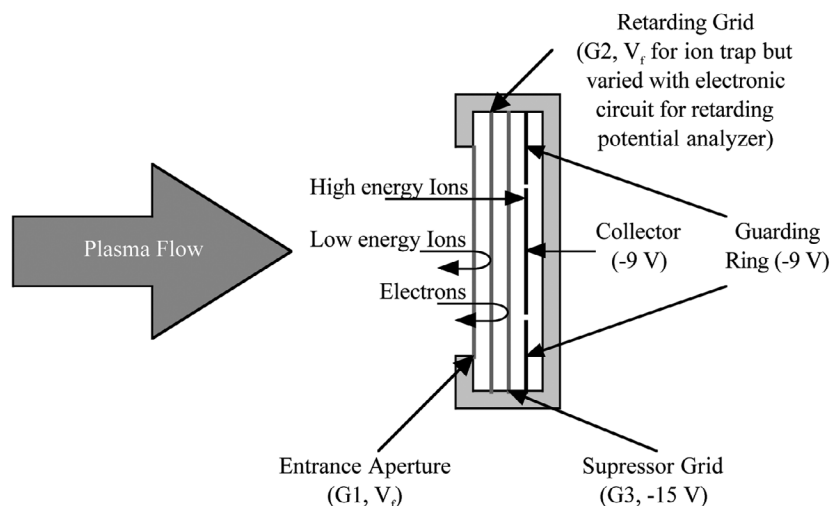The SR-V was launched at Jioupeng located in the southern part of Taiwan at 19:48:00 National Standard Time

Fig. 1. A cross section illustration of the ion probe onboard the SR-V.

(UT + 8) on 18 January 2006. It was directed at an elevation angle of 80° and at an azimuthal angle (~21°) between Green and Orchid Island. A high spin rate (~4 rps) was applied to maintain stability of the unguided rocket. Ground radars (a 30 MHz coherent scatter radar and a digisonde) were used to survey ionospheric plasma irregularities near the launch range. However, one of the digisondes close to the launch range failed around 4 hours before the rocket lifted off. The first stage of the rocket was separated at T + 5.7 s (~2.0 km altitude), where T is the launch time. The second stage was ignited successfully at T + 12.1 s (~5.0 km altitude) and then burned out at T + 43.3 s (~49.8 km altitude). The fairing opened at T + 58.1 s (~79.0 km altitude) with ground speed ~1.97 km s^{-1} as expected and the ion probes were then exposed outsides to measure ambient plasma. The rocket reached a maximum altitude of 281.1 km at T + 270.0 s in an inertial trajectory but under the effect of aerodynamic drag. An onboard GPS receiver and a 3-axis fluxgate magnetometer recorded its trajectory and attitude information (not a complete solution), respectively, during the flight. The telemetry was terminated at T + 512.8 s (~19.4 km altitude).

Ionospheric ions collected by the IT of the SR-V are represented as ion currents, I_{IT}, in Fig. 2. At the upleg (see Fig. 2a), a current spike (up to 1.8 nA) appears around 79.0 km altitude (T + 58.1 s). The spike is induced by apparent motion of the grids and the collector within the IT due to a vibration when the fairing opens, not a signal from ambient plasma. It was checked in a random vibration test at ground before the flight. Prominent currents (with level above 1 nA) are detected with two major peaks between 87.6 km (T + 62.6 s) and 112.3 km (T + 75.8 s) in the E region. The highest peak (~113.0 nA) is located at 93.0 km (T + 65.4 s) with a thickness of 3.4 km. The secondary peak (~27.1 nA) is located at 101.4 km (T + 69.9 s) with a wide coverage of 24.7 km for the whole region. It seems the highest peak is protruded from the secondary peak. We speculate the highest peak is related to a sporadic-E (E_s) layer and the secondary peak is more likely the E peak. These will be discussed in the final section of this article. Meanwhile, a small current spike (5.8 nA) is found at the upleg around 120.1 km (T + 80.2 s) but has a very narrow thickness/duration (17.5 m/0.01 s). It seems relative to a V_{G1} anomaly that will be described in later paragraphs.

As the SR-V goes up further, only small currents (lower than 1 nA) are detected up to 194.0 km (T + 130.3 s). Strip-like patterns are shown in the current readings and modulated with altitudes (or time) and current levels. They become remarkable in the low current level due to a switch between two different gains in a pre-amp circuit of the current
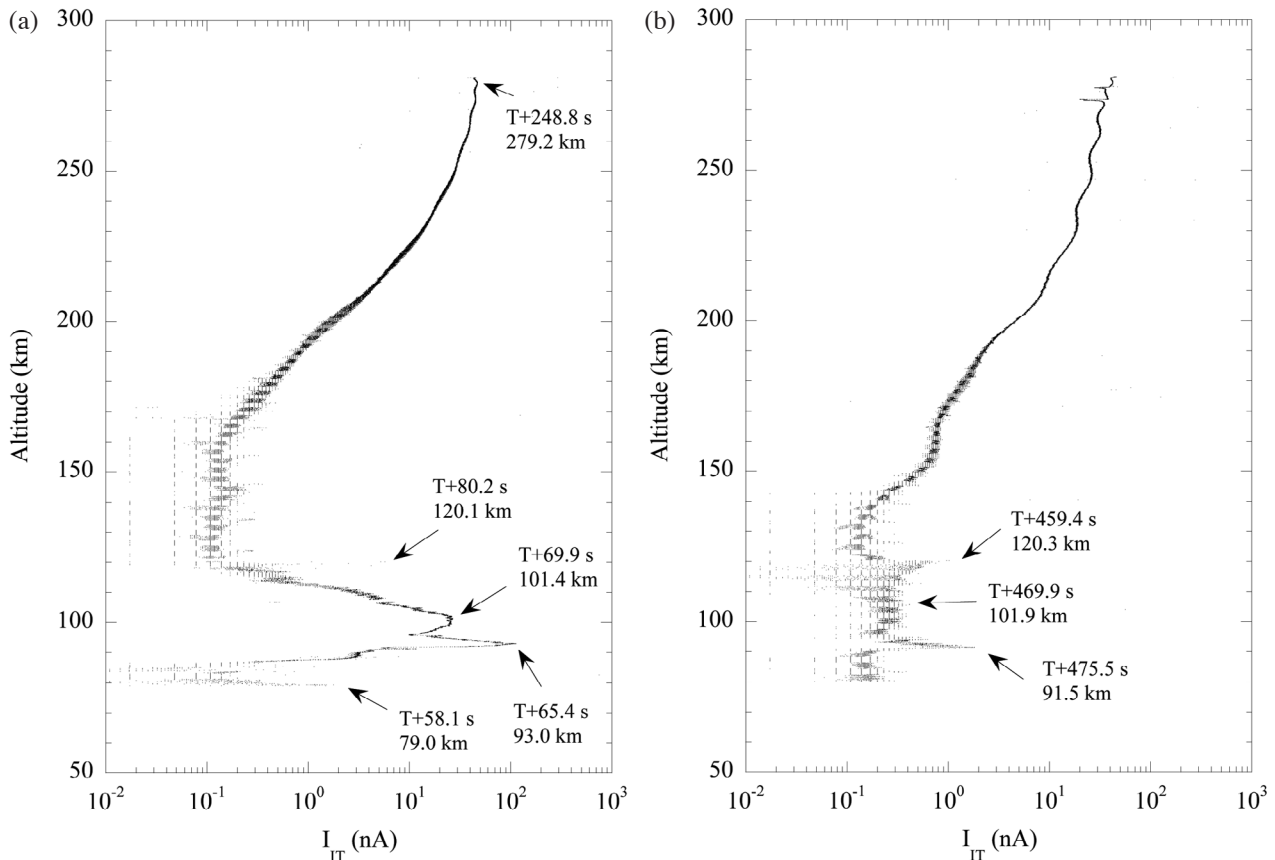

Fig. 2. Ion currents (I_{IT}) measured by the IT onboard the SR-V at the (a) upleg and (b) downleg.

meter every 1-second and a resolution limit of analog-to-digital converter in 16 bits for a current sample. Later, in the F region the I_{IT} increase with the altitudes and reach to a maximum (~47.5 nA) at 279.2 km (T + 248.8 s), which is very close to the maximum altitude of the test flight at 281.1 km. Near the maximum altitude, some undulations emerge in the current readings and are caused by coning motion of the rocket. It has been identified by the 3-axis fluxgate magnetometer installed on the rocket (not shown in this article).

At the downleg (see Fig. 2b), in the F region current undulations have greater perturbations than those at the upleg. On average, the I_{IT} are reduced when the rocket falls. Although the gain switch of the pre-amp circuit causes serious contamination in the current readings between 80 and 150 km altitude where most of the I_{IT} are lower than 1 nA, some features can be still identified as follows. When the SR-V approaches the E region, a small but significant current spike (~1.0 nA) is detected at 120.3 km (T + 459.4 s) with a thickness of 4.0 km. It is believed that the spike appears when the IT encounters an E_s layer. However, there is little correlation with the spike close to the similar altitude of the upleg. In a later time, a local current maximum (0.4 nA) is encountered at 101.9 km (T + 469.9 s) and suspected as an E peak, which is very close to the E peak (101.4 km) at

the upleg. Below the E peak, a strong current spike (1.8 nA) emerges at 91.5 km (T + 475.5 s) with a thickness of 4.1 km. It is also classified as an E_s layer and seems to resemble the one at the 93.0 km of the upleg. In the E region, the I_{IT} at the downleg are overall smaller than those at the upleg.

The V_{G2} readings of the RPA are presented in Fig. 3. At the upleg (Fig. 3a), the V_{G2} are triggered many times before the SR-V approaches the E region. First the V_{G2} readings are triggered by the vibration-induced I_{IT} (0.48 nA) at T + 58.1 s (79.0 km) when the fairing opens and then return back to -10 V after the vibration-induced I_{IT} are dampened. The V_{G2} are again triggered several times and return to -10 V soon, like at T + 60.6 s (83.9 km), at T + 61.3 s (85.2 km), etc. When the SR-V starts to contact the E region, the V_{G2} readings are triggered by the I_{IT} ~0.6 nA at 87.2 km (T + 62.4 s) and become stable at altitudes higher than 87.9 km (T + 62.7 s) with the I_{IT} ~2.1 nA. However, the V_{G2} readings fail to track for both the levels of 1/5 and 1/10 of the I_{IT}. The V_{G2} stay at +10 V until the SR-V reaches 98.6 km (T + 68.4 s). It implies that the I_{RPA} readings are always lower than 1/10 of the I_{IT} at that moment. However, the V_{G2} gradually return to -10 V at 98.6 km (T + 68.4 s) even the I_{IT} is as high as the 21.2 nA. The reason is unknown and will be left for future study. After the SR-V reaches the F region, the V_{G2} start triggering but highly fluctuating at 192.7 km (T + 123.0 s)

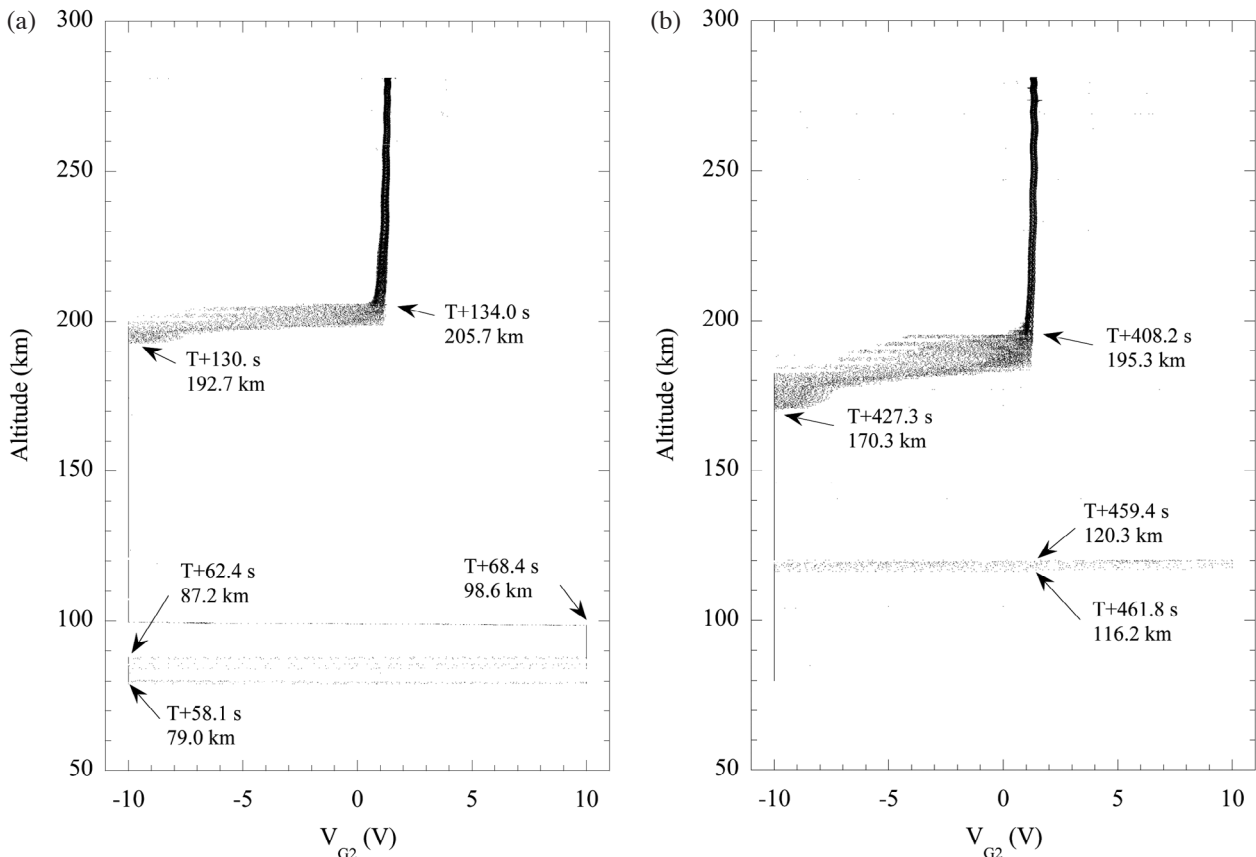Fig. 3. Retarding voltages (V_{G2}) measured by the RPA onboard the SR-V at the (a) upleg and (b) downleg.

where the I_{IT} ~1.0 nA. The V_{G2} become stable switching between 0.40 and 1.14 V at the altitudes higher than 205.7 km (T + 140.0 s) where the I_{IT} > 2.8 nA.

At the downleg (see Fig. 3b), the V_{G2} maintain the stable condition until the SR-V falls to 195.3 km (T + 408.2 s) where the V_{G2} switching between 0.46 and 1.29 V and the I_{IT} ~3.1 nA. And then the V_{G2} become highly fluctuated toward negative values and cease at -10 V at 170.3 km (T + 427.3 s) where the I_{IT} have dropped to 0.9 nA. When the SR-V falls further into the E region, the V_{G2} are triggered at 120.3 km (T + 459.4 s) where the I_{IT} ~0.4 nA and cease at 116.2 km (T + 461.8 s) where the I_{IT} ~0.4 nA.

The stable V_{G2} patterns in the F region can be used to derive the ion temperature in the future. However, no useful V_{G2} readings can be used to determine the ion temperature even though very high I_{IT} (> 1 nA) readings have been detected in the E region at the upleg.

Although the E_s layers are successfully detected during the SR-V flight, an anomaly in the V_{G1} found in the E region at the upleg (see Fig. 4a) implies more complex situations. From the telemetry, the V_{G1} readings are almost zero when the ion probes are preserved in the fairing. When the fairing opens, the G1 suffers the vibration to make the V_{G1} jump up to 0.21 V immediately and then recover to zero in 1.5 s as

the vibration becomes attenuated. At 83.7 km (T + 60.5 s), the V_{G1} readings suddenly but continuously drop from 0 to -10 V and maintain at -10 V until to 120.1 km (T + 80.2 s). It is noted that the V_{G1} readings are limited within ±10 V, which are the extreme output voltage range of the analog-to-digital converter. However, the V_{G1} seems to fall between -10 and -15 V, which is the lowest voltage provided by a voltage regulator in the ion probes. The V_{G1} become normal after the 19.7-s anomaly and start increasing from 0 to positive values with the altitudes. The V_{G1} go up to 0.40 V at 279.1 km (T + 248.5 s) very close to the maximum altitude of the test flight.

At the downleg, no anomaly in the V_{G1} is found like the case at the upleg. The V_{G1} remain positive but become small as the SR-V falls. As the SR-V approaches nearby the E_s layer at 120.3 km, the V_{G1} increase up to 0.19 V and back to 0 V after the SR-V passes through it. As the SR-V falls further to the other E_s layer at 91.5 km, the V_{G1} increase up to 0.01 V and return to 0 V soon.

The anomaly in the V_{G1} is speculated as a short circuit between the G1 and the G3 occurring right after the fairing separation. The G2 is probably shortened with the two grids together. The collector remains open to the grids; otherwise a strong negative current should be detected. According to
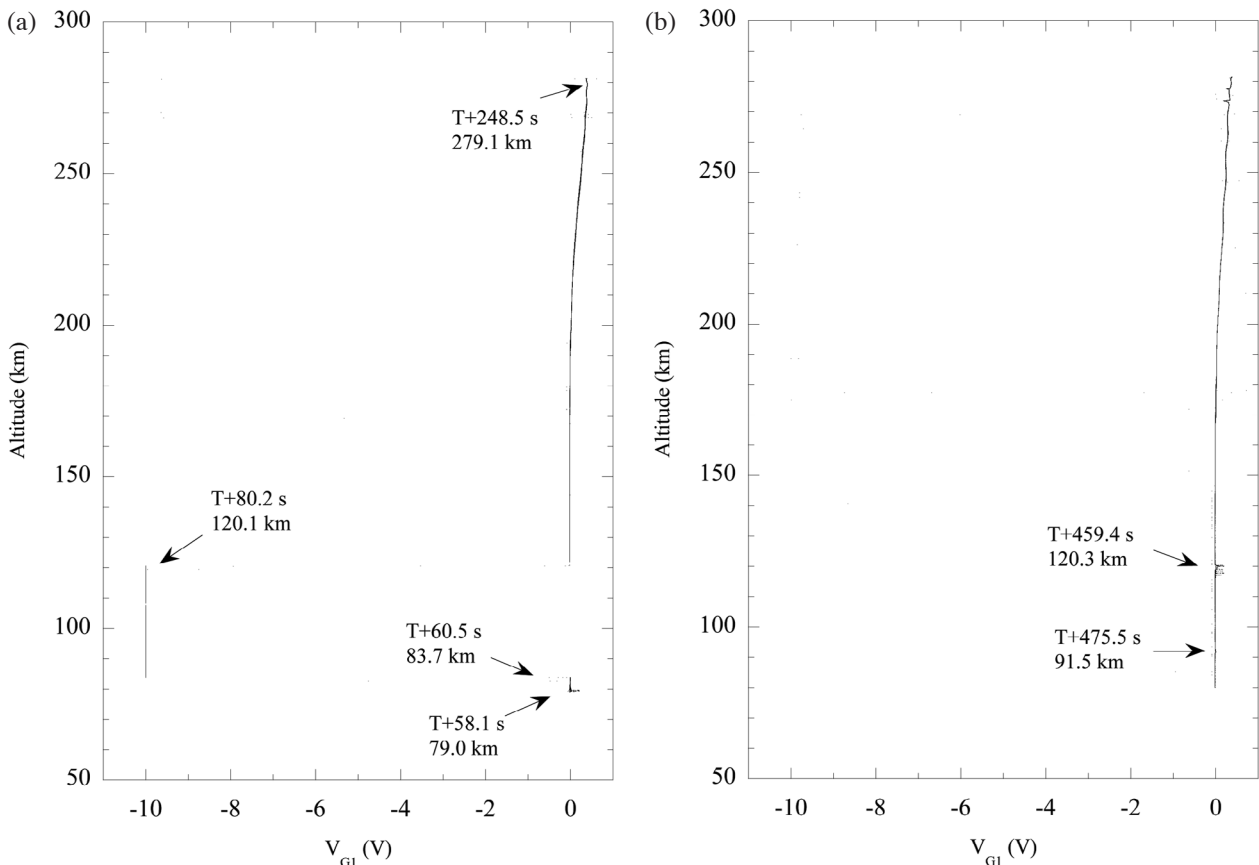

Fig. 4. The V_{G1} variation measured by the IT onboard at the up-leg of the SR-V at the (a) upleg and (b) downleg. One anomaly is shown in the V_{G1} to drop down to -10 V at the altitudes between 83.7 and 120.1 km at the upleg.

this scenario, the V_{G1} are biased by the G3 to -15 V and the voltage readings become -10 V due to the limit of the analog-to-digital converter. One hypothesis for this anomaly is that the metal grids of the IT are deformed by outflowing air. The tension of the metal grids is quite low after inspecting an IT engineering model of the SR-V. The grids contact each other after the fairing opens and then restore to be normal (open circuit) in later time. Before the flight the ion probes are air-sealed in the fairing and purged with dry nitrogen gas continuously at pressure slightly higher than 1 atm to prevent contamination from water vapor. Another hypothesis is a conductor (especially a metal wire) dropped into the IT after the fairing opens. Pinhole cameras installed in the fairing indicate some tiny objects appear when the fairing opens. The conductor is probably jammed between the G1 and the G3 of the IT to let V_{G1} be -15 V. After the 19.7 s, the conductor may be blown up and the V_{G1} become normal.

The consequence of the anomaly in the V_{G1} results in changes of the I_{IT} collection by plasma sheath expansion around the opening of the IT. Abrupt changes in the I_{IT} should appear at the T + 60.5 s and the T + 80.2 s, when the V_{G1} drop from 0 to -15 V and return from -15 to 0 V, respectively. However, at those moments the current readings are around the noise level of the current meter. No clear current changes are observed to evaluate the effect caused by the anomaly in the V_{G1}. Laboratory simulations are required to estimate the I_{IT} differences for the V_{G1} at 0 and -15 V.

3. LABORATORY SIMULATIONS

A Space Plasma Simulation Chamber (SPSC) started operation at Space Payload Laboratory, National Central University in June 2007 to develop and test space payloads in a plasma environment like terrestrial ionosphere. The cylindrical chamber is made of T304 stainless steel to reduce the magnetic field caused by the chamber. The interior space is 700 mm in diameter and 1500 mm in length (see Fig. 5a). Two 850-mm doors and twelve 6-in openings (V_{G1}50) on the side are used to access and provide feedthroughs to the chamber.

Chamber pressure is monitored by a Pirani vacuum gauge in a low vacuum stage (between 0.4 and 2700 Pa) and an ionization gauge in a high vacuum stage (between 1.3 × 10^{-5} and 0.67 Pa). Vacuum pumps are serially connected to one of the chamber openings and evacuated the gases in the chamber to air. A direct-drive oil sealed rotary vacuum pump with a pumping speed at 240 L min^{-1} is used as a foreline/backing pump to reduce the chamber pressure from 1 atm to 10 Pa. A compound molecular turbo pump with a speed of 750 L s^{-1} is used as a high vacuum pump to reduce the pressure from 300 Pa to high vacuum. These pumps are manually operated and usually take 8 hours to reduce the chamber pressure from 1 atm to 10^{-6} torr. A clamp valve of automatic leak type is installed in between the rotary pump and turbo pump to prevent inner surface of the chamber from oil contamination once power outage.

A back diffusion plasma source is installed in the door with a 10-inch opening (VG250). The source produces plasma with a density around 10^3 to 10^6 # cm^{-3} and temperature around 1000 to 2000 K in a thermal ionization process. The plasma source contains replaceable nickel filaments in parallel connection, two acceleration grids, and one back plate as illustrated in Fig. 5b (but not in a real scale). All the grids and the plate are made of T304 stainless steel. Barium carbonate is coated on the filaments and must be activated first.
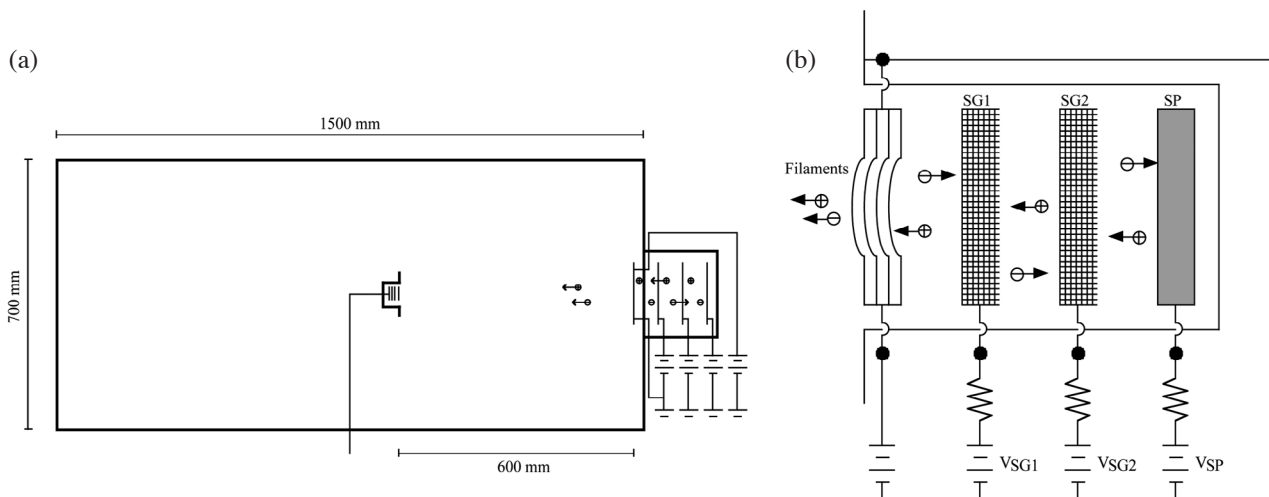

Fig. 5. (a) Schematic of a space plasma simulation chamber and (b) a back diffusion plasma source at the Space Payload Laboratory, National Central University. A back diffusion plasma source is installed in the right-hand side to release plasma toward an IT located at the center of the chamber. The filaments are located at the opening. SG1, SG2, and SP are applied at high positive voltages, V_{SG1}, V_{SG2}, and V_{SP}, respectively, referenced to chamber body.

By conducting sufficient electric currents (~several amperes for one filament) through the filaments to red in a slow pace, the coating on the filaments is gradually reacted to release carbon dioxide and become barium oxide. The activated coating has a low work function to allow more electrons escaped from its thermal surface.

The escaped electrons are attracted and accelerated toward inner space of the plasma source by the first acceleration grid (SG1) that is applied to a positive voltage (V_{SG1}). The electrons are further accelerated toward the back plate by the second acceleration grid (SG2) that is applied to a higher positive voltage (V_{SG2}). The back plate (SP) is applied to the highest positive voltage (V_{SP}) and also used to stop the electron motions. In the process the electrons collide with released neutral gases and produce new electron-ion pairs. The produced ions are then accelerated toward the filaments and can carry the electrons out of the source together due to the heavy mass of the ions in an ambipolar diffusion process. The accelerated plasma has a high mean flow in the chamber. The mean velocity can be estimated by the electric potentials (V_{SG1}, V_{SG2}, and V_{SP}) of the grids and plate.

In laboratory simulations, an IT engineering model of the SR-V is installed on a turntable to align the probe opening to normal (as in Fig. 5a) or perpendicular to the plasma source. The G1 and the G2 of the IT are electrically connected to a power supply. The power supply can adjust its output to provide negative voltages on the grids. Collector currents are converted to voltage signals by a pre-amp circuit and recorded by a high-precision 16-bit digital acquisition board. The G3 is maintained at -15 V and the collector at -9 V as the flight model. All the voltages are grounded to the chamber body and electrical outlets of the laboratory building. Argon gas is released to the chamber at a pressure around 1.08×10^{-2} Pa. The gas release is regulated by a digital mass flow meter/controller with ±1% accuracy in flow rate. The coating on the filaments is slowly activated to make the plasma flow reach to a stable condition. The biased voltages of the back diffusion plasma source are tuned at 100 V for V_{SG1}, at 130 V for V_{SG2}, and at 200 V for V_{SP}. The mean flow speed is estimated ~27 km s^{-1} from the voltages of the grids and plate. It is much higher than the ion thermal velocity (0.56 km s^{-1}) in the chamber if a typical ion temperature 1500 K is applied.

In this experiment two extreme cases are performed and their results are shown in Fig. 6. One is to align the opening of the IT to face the plasma source. As the voltages on the G1 and the G2 decrease from 0 to -15 V in a voltage step of -2.5 V, the I_{IT} (a solid line) received at the collector increase rapidly from 63.3 nA to a saturated level (~126.0 nA) after -10 V. It is noted that standard deviations of the I_{IT} are too small to identify in the figure. The result indicates that the I_{IT} for the V_{G1} at -15 V is 98.4% more than that at 0 V. It can be foreseen that negative voltages on the G1 result

in plasma sheath expansion around the opening of the IT. Additional ions can fall into the sheath region from side and are attracted into the IT. The result also indicates that the plasma sheath expansion is effective at low negative voltages but limited at high negative voltages.

The other case is to rotate the opening of the IT perpendicular to the plasma source. The variation of the I_{IT} (a dashed line) is similar to the previous case but the I_{IT} are lower as expected. A very small ion current (~1.17 nA) is collected for the V_{G1} at 0 V. It is because mean plasma flows are unable to go into the IT directly. Only a small fraction of plasma can thermally diffuse into the collector. Once the G1 and G2 are applied to high negative voltages, the plasma sheath expansion allows more ions to slide into the IT. The I_{IT} reach to a maximum (~56.7 nA) for the V_{G1} at -12.5 V. At higher negative voltages the incoming ions caused by the plasma sheath expansion are limited but some of them hitting on the G1 and G2 are lost. The effect can only be analyzed in a simulation model (Chao et al. 2003). The I_{IT} for the V_{G1} at -15 V is 4580% more than that at 0 V. It can reinforce the first case that the plasma sheath expansion plays an important role in the current collection.

4. DISSCUSSION AND SUMMARY

According to ion temperature and species provided by the IRI-2001 model (Bilitza 2001) under the launch conditions (including time, location, solar flux, magnetic index, etc.), E-region total ion concentration (N_i) profiles could be derived from the I_{IT}. The derivations are based on a one-dimensional ion flux equation (Whipple 1959) with consideration of the angle of arrival for the ions into the IT. However, the effects of the coning motion and the spinning of the rocket are not excluded from the data. A small coning
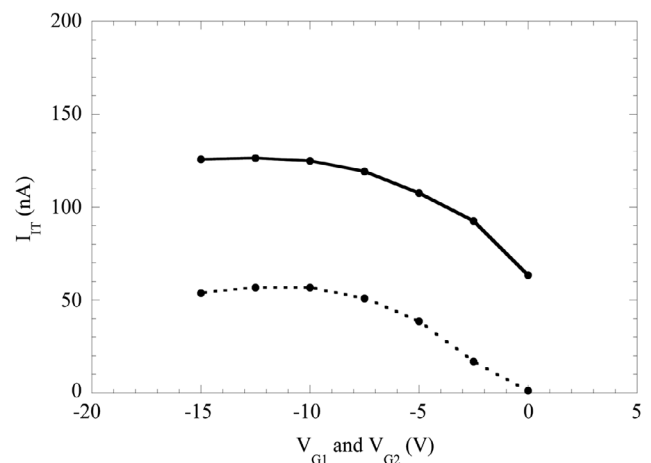
Fig. 6. Ion currents (I_{IT}) measured by an engineering model of the ion probe for the SR-V with voltages on G1 and G2 for the probe opening face to (a solid line) and perpendicular (a dash line) to the plasma source.

motion has been detected by the 3-axis fluxgate magnetometer in the inertial flight of the SR-V. The coning angle of the rocket is less than 10° and the period around 21 s. It suggested that no dramatic attitude changes when the SR-V passes through the E region. As for the effect of the spinning, it can be easily identified from those variations around 4 Hz. Hopefully the variations caused by the spinning are small and do not alter the large-scale N_i profiles much. The calibration processes for these attitude modulations will be investigated in the future work.

Un-calibrated N_i profiles are represented in black dots in Fig. 7. At the upleg (see Fig. 7a), the E_s layer at 93.0 km altitude has an un-calibrated peak density of about 1.9×10^5 # cm^{-3}. It should be noted here that the density is over-estimated and will be described in the following paragraphs. At the first glance, it seems common for the E_s layers observed in many sounding rocket missions. Like the SEEK-1 campaign (Yamamoto et al. 1998), the main E_s layer has a peak density of around 8.0×10^4 cm^{-3} at 98 km at the upleg and 6.5×10^4 cm^{-3} at 100 km at the downleg. In the SEEK-2 campaign (Wakabayashi et al. 2005), the main E_s layer had a peak density 9.5×10^4 cm^{-3} at 104.6 km at the upleg and 4.7×10^4 cm^{-3} at 102.6 km at the downleg. However, the

E_s layers detected by the SR-V should have weaker density profiles. It is because the E_s layers were diminishing during the rocket launch. The 30 MHz radar discovered the plasma irregularities around 18:00 LT and had the strongest echo around 18:30 LT. The echo becomes weaker and ceases at 20:50 LT (not shown in this article).

Meanwhile, the un-calibrated E-peak density is about 4.6×10^4 # cm^{-3}, which is much higher than that (~1.7×10^3 # cm^{-3}) estimated by the IRI-2001 model. The local sunset above the launch range at 100 km altitude is 18:19 LT. Even though the sunset time at its conjugate point is around 19:27 LT, it is slightly early than the observation time around 19:49 LT. The main ion species, like NO$^+$, O$_2^+$, and N$_2^+$, have very high dissociative recombination loss rates in the nighttime E region (Rishbeth and Garriott 1969). The E-region plasma should diminish in several ten seconds after the sunset. Even the other ionization sources, like starlight and resonantly scattered solar radiation (H Lyman α and β) are considered, the observable electron density has an order of 1×10^3 to 4×10^3 # cm^{-3} in the true nighttime conditions (Strobel et al. 1980; Schunk and Nagy 2009). Therefore, the un-calibrated E-region N_i profile derived at the upleg is too high to sustain in the nighttime.
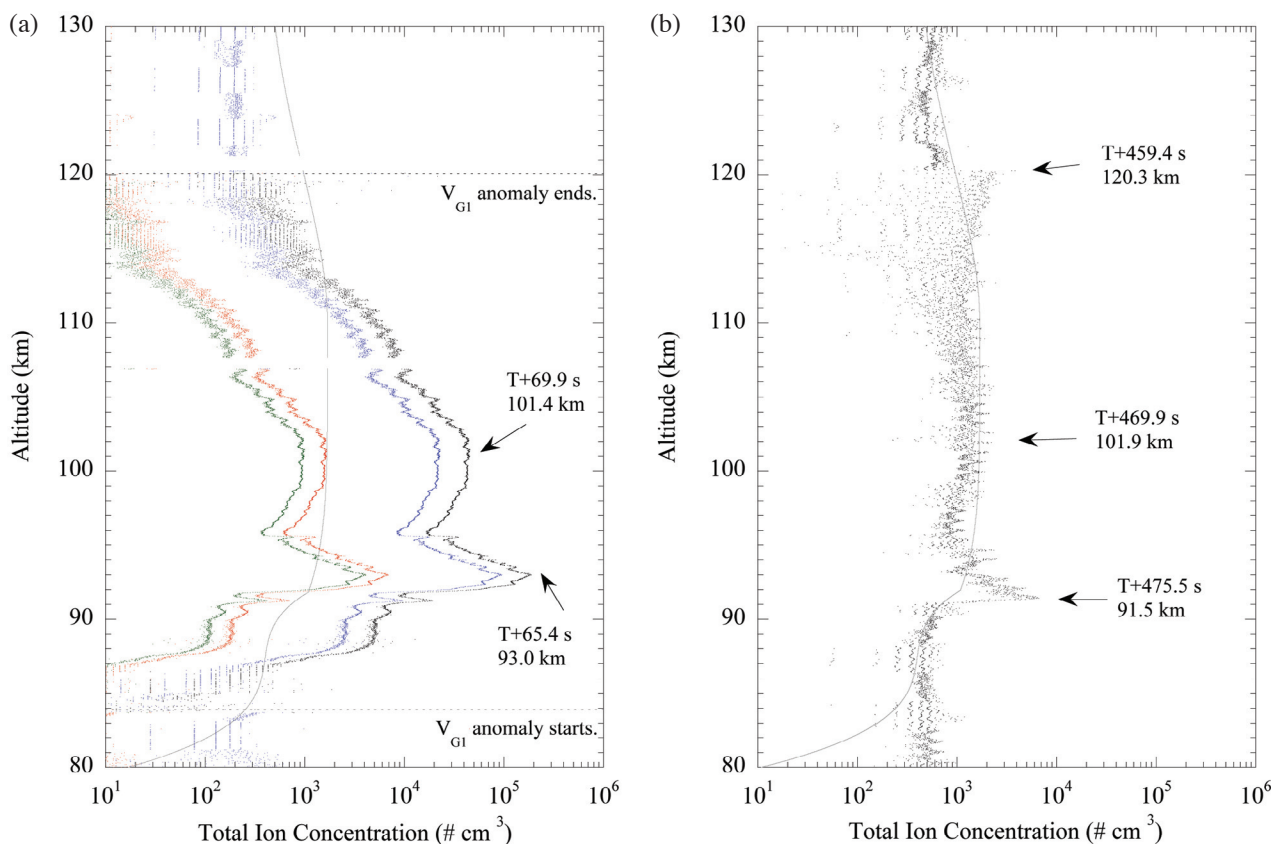

Fig. 7. Total ion concentration (N_i) profiles derived from the I_{IT} measured by the SR-V at the (a) upleg and (b) downleg. The gray lines indicate the N_i profiles derived from the IRI-2001 model. The dashed lines indicate the start and end altitude for the V_{G1} anomaly. At the upleg the un-calibrated N_i profile is plotted in black dots. The calibrated N_i profiles are plotted in green, blue, and red dots for using scale factors from the lab simulations with the probe perpendicular/face to the plasma source, and from the IRI-2001 model.

At the downleg (see Fig. 7b), the N_i derived from the I_{IT} match the IRI-2001 model (in gray lines) well near the E peak (~101.9 km) with an average density of about 1.4×10^3 # cm^{-3} despite some fluctuations (with an uncertainty of ~10^2 # cm^{-3}) caused by the spinning rocket. The E_s layers are clearly shown at 91.5 and 120.3 km altitude with density 6.6×10^3 # cm^{-3} and 3.8×10^3 # cm^{-3}, respectively. This information conform our understandings of the E region and E_s layer at night and stimulate some methods to calibrate the E-region N_i profile at the upleg.

The anomaly in the V_{G1} leads to the extraordinarily high I_{IT} in the E region at the upleg. The un-calibrated E-region N_i profile at the upleg is then over-estimated. It also makes the I_{IT} always higher than the I_{RPA} and no V_{G2} square wave patterns are available in the E region like in the F region.

Although a numerical model has been used to study charged particle motions (Chao and Su 2000) and grid effects (Chao et al. 2003) for an ion probe, it can only be used to evaluate the charged particle scattering by the high negative voltage grids. The effect of the plasma sheath expansion is out of scope of this model. The charged particle scattering for the anomaly in the V_{G1} only accounts ~18% in additional currents for the SR-V flight condition. The effect is quite smaller than the 98.4% for the probe faced to the source or 4580% for the probe perpendicular to the source in the laboratory simulation. The plasma sheath expansion produced by the high negative V_{G1} is probably the main cause to collect extra ions into the IT. The un-calibrated E-region N_i profile can be scaled down by factors of 1.98 and 46.8 derived from the laboratory simulation to reflect two possible extreme profiles (see Fig. 7b) shown in blue and green dots, respectively. The real solution of the N_i profile may converge within these two profiles. However, the possible profile is most likely the case for the IT facing to the plasma source instead of perpendicular to it from this study. It is because the ground speed (~1.97 km s^{-1} at 100 km altitude) of the SR-V is much higher than the ion thermal velocity (~0.31 km s^{-1} for NO^+ with temperature 350 K).

Another way to estimate the scale factor is to use the IRI-model. Since the derived N_i profile is so similar to the model at the downleg, it suggests that the un-calibrated N_i profile can be scaled with the E peak density (1.7×10^3 # cm^{-3}) from the IRI model. A factor of 27.3 is used to calibrate the N_i profile (see Fig. 7b) shown by red dots. It is well bound between the two extreme cases from the laboratory simulations. The scale factor is also satisfied in that the I_{RPA} are always lower than 1/10 of the I_{IT} when the anomaly in the V_{G1} is encountered. The calibrated N_i profile at the upleg indicates the peak density of the E_s layer at 93.0 km altitude is about 6.9×10^3 # cm^{-3} with a thickness of 3.4 km. It is very similar to that at 91.5 km altitude has a density of 6.6×10^3 # cm^{-3} with a thickness of 4.1 km at the downleg. It is the best solution for the E-region N_i profile at the upleg. It implies that the E_s layer has a wide coverage and the SR-V

might encounter the same E_s layer twice in a distance of 150 km away.

Although the probes did not perform flawlessly in the flight test, the anomaly in the V_{G1} gives us some hints to measure a very low plasma density in the present circuit architecture if a careful calibration is applied. The V_{G1} can be applied to a high negative voltage to expand the plasma sheath to collect more plasma into the probe.

REFERENCES

Bilitza, D., 2001: International reference ionosphere 2000. *Radio Sci.*, **36**, 261-275, doi: 10.1029/2000RS002432. [Link]

Boyd, F. L. F., 1968: Langmuir probes on spacecraft. In: Lochte-Holtgreven, W. (Ed.), Plasma Diagnostics, North-Holland Publishing Co., Amsterdam, 732-776.

Chao, C. K. and S. Y. Su, 2000: Charged particle motion inside the retarding potential analyzer. *Phys. Plasmas*, **7**, 101-107, doi: 10.1063/1.873817. [Link]

Chao, C. K., S. Y. Su, and H. C. Yeh, 2003: Grid effects on the derived ion temperature and ram velocity from the simulated results of the retarding potential analyzer data. *Adv. Space Res.*, **32**, 2361-2366, doi: 10.1016/S0 273-1177(03)90566-7. [Link]

Chu, Y. H., C. L. Su, M. F. Larsen, and C. K. Chao, 2007: First measurements of neutral wind and turbulence in the mesosphere and lower thermosphere over Taiwan with a chemical release experiment. *J. Geophys. Res.*, **112**, A02301, doi: 10.1029/2005JA011560. [Link]

de La Beaujardière, O. and the C/NOFS Science Definition Team, 2004: C/NOFS: A mission to forecast scintillations. *J. Atmos. Sol.-Terr. Phys.*, **66**, 1573-1591, doi: 10.1016/j.jastp.2004.07.030. [Link]

Heelis, R. A. and W. B. Hanson, 1998: Measurements of thermal ion drift velocity and temperature using planar sensors. In: Pfaff, R. F., J. E. Borovsky, and D. T. Young (Eds.), Measurement Techniques in Space Plasmas: Particles, American Geophysical Union Monograph, 61-71.

Minami, S., S. Tsutsumi, and Y. Takeya, 1982: Graphical analysis method for a retarding potential analyzer and its application to the real-time measurements of ion temperature in space plasmas. *Rev. Sci. Instrum.*, **53**, 1709-1713, doi: 10.1063/1.1136874. [Link]

Rishbeth, H. and O. K. Garriott, 1969: Introduction to Iono-

spheric Physics, Academic Press, New York, 87-125.

Schunk, R. W. and A. F. Nagy, 2009: Ionospheres: Physics, Plasma Physics, and Chemistry, Cambridge University Press, Cambridge, 352-353.

Strobel, D. F., C. B. Opal, and R. R. Meier, 1980: Photoionization rates in the night-time *E*- and *F*-region ionosphere. *Planet. Space Sci.*, **28**, 1027-1033, doi: 10.10 16/0032-0633(80)90050-1. [Link]

Wakabayashi, M., T. Ono, H. Mori, and P. A. Bernhardt, 2005: Electron density and plasma waves in mid-latitude sporadic-*E* layer observed during the SEEK-2 campaign. *Ann. Geophys.*, **23**, 2335-2345, doi: 10.5194/ angeo-23-2335-2005. [Link]

Whipple, E. C., Jr., 1959: Exploration of the upper atmosphere with the help of the third Soviet Sputnik. *Proc. IRE*, **47**, 2023-2024.

Yamamoto, M., T. Ono, H. Oya, R. T. Tsunoda, M. F. Larsen, S. Fukao, and M. Yamamoto, 1998: Structures in sporadic-*E* observed with an impedance probe during the SEEK campaign: Comparisons with neutral-wind and radar-echo observations. *Geophys. Res. Lett.*, **25**, 1781-1784, doi: 10.1029/98GL00709. [Link]

Yeh, H. C., S. Y. Su, Y. C. Yeh, J. M. Wu, R. A. Heelis, and B. J. Holt, 1999: Scientific mission of the IPEI payload onboard ROCSAT-1. *Terr. Atmso. Ocean. Sci.*, **10 (Suppl.)**, 19-42.